SCIENCE CHINA
Physics, Mechanics & Astronomy

• Research Paper •

February 2010 Vol. 53 No. 2: 360–368
doi: 10.1007/s11433-010-0124-z

Series solution of non-similarity natural convection boundary-layer flows over permeable vertical surface†

KOUSAR Nabeela & LIAO ShiJun*

State Key Lab of Ocean Engineering, School of Naval Architecture, Ocean and Civil Engineering, Shanghai Jiao Tong University, Shanghai 200240, China

Received October 10, 2009; accepted October 28, 2009

The non-similarity solution for natural convection from a permeable isothermal vertical wall is considered. The governing boundary-layer equations for non-similarity flow and temperature fields are solved using the homotopy analysis method. The homotopy-Padé technique is applied to accelerate the convergence of the homotopy-series solution. The influence of physical parameters on the non-similarity flows is investigated in detail. Different from the previous analytic results, the homotopy-series solutions are convergent and valid for all physical parameters in the whole domain $0 \leqslant x < \infty$ and $0 \leqslant y < \infty$.

non-similarity, porous surface, natural convection, boundary-layer flow, homotopy analysis method

Natural convection has attracted a great deal of attention because of its presence both in nature and engineering applications. In nature, convection cells, formed from air raising above sunlight warmed land or water, are a major feature in all weather systems. In engineering applications, convection is commonly visualized in the formation of microstructures during the cooling of molten metals, and fluid flows around shrouded heat-dissipation fins, and solar ponds. A very common industrial application of natural convection is free air cooling without the aid of fans. Many free convection processes occur in environments with temperature stratification. The buoyant flow arising from heat rejection to atmosphere, heating of rooms, fires, and many other such heat transfer processes, both natural or artificial, are the examples of natural convection flows.

Several attempts have been made in recent years to investigate the problem of natural convection over a vertical wall in a stratified medium due to its obvious importance. Early studies focused on seeking similarity solution because the similar variables can give great physical insight with minimal efforts. Cheesewright [1] obtained the similarity solutions of various types of non-uniform ambient temperature distributions by a theoretical investigation of laminar free convection from a vertical plane in non-isothermal surroundings. Eichhorn [2] studied the effect of linear thermal stratification on the heat transfer of an isothermal vertical plate and obtained solutions for four terms of the series expansions of the partial differential equations. Subsequently, Fujii et al. [3] considered the effect of non-linear thermal stratification on the problem of Eichhorn [2] and gave solutions for four terms of the series expansions. Later, Chen and Eichhorn [4] reconsidered the problem of Eichhorn [2] and obtained solutions using the local non-similarity method. Yang et al. [5]investigated the natural convection heat transfer from a non-isothermal vertical flat plate immersed in a thermal stratified medium. Venkatachala and Nath [6] solved the complete set of governing partial differential equations for the problem of an isothermal wall in linearly stratified atmosphere using the implicit finite-difference scheme, perturbation series expansion and local non-similarity method. They compared their results with Chen and Eichhorn [6] and found very good agreement with small Pr and large x/L. Jaluria and Himasekhar [7] studied the problem of natural convection flow in a plane thermal plume and the flow over a heated vertical plate in an arbitrary, but stably stratified environment and gave the numerical solutions of the governing partial differential equations by using the finite difference method for two values of the Prandtl

* Corresponding author (email: sjliao@sjtu.edu.cn)

† Contributed by LIAO ShiJun

number 0.72 and 6.7 for air and water, respectively, at normal temperature. Kulkarni et al. [8] investigated the problem of natural convection from an isothermal flat plate suspended in a linearly stratified fluid using the Von-Karman-Pholhausen integral solution method. They obtained the similarity solutions for two cases, the classical one (T_w, T_∞ = const), and the case where T_w = const and $T_w(x)$ is linear and stable. The same problem was then investigated experimentally by Tanny and Cohen [9], who found that the heat and local heat transfer is in good agreement with the theoretical predictions done by Kularni et al. [8].

A problem of interest and importance in some applications concerns the effect of blowing and suction in a natural convection boundary-layer. This situation would arise, for instance, if heat from a porous surface were being investigated and fluid were being added to or removed from the flow. Kao [10] applied the shooting method technique to solve the non-similarity boundary-layer and thermal boundary-layer equations for the forced convection along a flat plate with arbitrary suction or injection at the wall. For the flat plate with suction Emmons and Leigh [11] found solutions of the momentum equation, while the corresponding heat transfer results for the isothermal porous plate were presented by Schilichting and Bussemann [12].

For similarity boundary-layer flows, velocity profiles at different x are *similar*. However, such kind of similarity is lost for non-similarity flows [13–15]. Briefly speaking, the non-similarity boundary layer flows are more general in nature and in our everyday life, and thus are more important than the similarity ones. For the non-similarity solution, one had to solve a system of nonlinear partial differential equations (PDEs). Mathematically, it is more difficult to solve PDEs than ordinary differential equations (ODEs). Most of the solutions of the boundary-layer equations have been numerically obtained. Numerical methods can be used to approximate the results at large numbers of discretized points. However, it brings some additional errors and uncertainty into the numerical results when infinite domain is replaced by the finite ones. The PDEs can be solved in the infinite domain by using the traditional analytic methods. But, the results obtained by these traditional methods are not valid for all physical parameters in the whole domain because these techniques, more or less, depend on the small/large physical variables. In recent years, among the analytic methods for non-similarity thermal boundary-layer problems, "the method of local non-similarity" seems to be most frequently applied. However, the results given by this method are of uncertain accuracy and only valid for small ξ [16–18].

Previous studies show that no one has found the non-similarity solution for natural convection flow from the permeable vertical surface in an isothermal surroundings. Precisely, we have undertaken this task successfully and described it in this paper. We obtained the explicit series solution for natural convection flow over an isothermal vertical porous wall by means of homotopy analysis method (HAM). The HAM is a general analytic approach to get series solutions of various types of non-linear equations, including algebraic equations, ODEs, PDEs, differential-integral-equations, differential-difference equation, and coupled equations of them. Different from perturbation techniques [19], the HAM does not depend upon any small/large physical parameters. Besides, it logically contains other non-perturbation techniques such as Lyapunov's small parameter method [20], the δ-expansion method [21], and Adomian's decomposition method [22], as proved by Liao in his book [23]. The HAM has been successfully applied to various nonlinear problems in science and engineering, such as nonlinear heat transfer [24–26], finance problems [27,28], projectile motion [29], groundwater flows [30], thermal-hydraulic networks [31] and so on. Especially, some new solutions of a new nonlinear equations are obtained [32,33]: theses new solutions have never been reported by all other previous analytic methods and even by numerical methods. All of these illustrate the great potential and flexibility of the HAM for strongly nonlinear problems in science and engineering.

1 Mathematical formulations

Let us consider the steady two-dimensional laminar boundary-layer flow along the permeable vertical surface in an isothermal surroundings. Let x denote the distance along the surface from the leading edge and y is the normal distance from the surface. With the Boussinesq assumption, i.e. assuming the density variation to be important only in the buoyancy term, the equations of continuity, momentum and energy, which govern the flow and heat transfer in a laminar boundary-layer are

$$\frac{\partial u}{\partial x} + \frac{\partial v}{\partial y} = 0\,, \tag{1}$$

$$u\frac{\partial u}{\partial x} + v\frac{\partial u}{\partial y} = g\beta(T - T_\infty) + \nu\frac{\partial^2 u}{\partial y^2}\,, \tag{2}$$

$$u\frac{\partial T}{\partial x} + v\frac{\partial T}{\partial y} = \alpha\frac{\partial^2 T}{\partial y^2}, \tag{3}$$

subject to the boundary conditions:

$$\begin{aligned} &y = 0 \;: \quad u = 0, \quad v = bx^n, \quad T = T_{\rm w}, \\ &y \to \infty \;: \quad u = 0\,, \quad \text{and} \quad T = T_\infty, \end{aligned} \tag{4}$$

respectively, (u, v) are the velocity components along the (x, y) axes, g is the gravitational acceleration, β is the coefficient of thermal expansion, α is the thermal diffusivity and ν is the kinematic viscosity. These equations may be nondimensionalized by employing a characteristic dimension, which gives rise to the Grashof number Gr.

The nondimensionalization employed here is given by the

following variables

$$\begin{aligned} &X = \frac{x}{L}, \quad Y = \frac{y}{L}, \quad U = \frac{uL}{\alpha}, \quad V = \frac{vL}{\alpha}, \\ &\Psi = \frac{\psi}{\alpha}, \quad Pr = \frac{\nu}{\alpha}, \quad \theta = \frac{T - T_\infty}{T_\mathrm{w} - T_\infty}, \\ &Gr = \frac{g\beta(T_\mathrm{w} - T_\infty)L^3}{\nu^2}, \end{aligned} \tag{5}$$

where L is the characteristic length such that when $x = L$, $T_\infty = T_\mathrm{w}$. With the above dimensionless variables, the governing equations become

$$\frac{\partial U}{\partial X} + \frac{\partial V}{\partial Y} = 0, \tag{6}$$

$$U\frac{\partial U}{\partial X} + V\frac{\partial U}{\partial Y} = GrPr^2\theta + Pr\frac{\partial^2 U}{\partial Y^2}\ , \tag{7}$$

$$U\frac{\partial \theta}{\partial X} + V\frac{\partial \theta}{\partial Y} = \frac{\partial^2 \theta}{\partial Y^2}, \tag{8}$$

with the boundary conditions

$$\begin{aligned} &Y = 0 \qquad U = 0, \quad V = aX^n, \quad \theta = 1, \\ &Y \to \infty \quad U = 0, \quad \text{and} \quad \theta = 0. \end{aligned} \tag{9}$$

where $a = \dfrac{bL^{n+1}}{\alpha}$. Using the transformations as mentioned in [8]:

$$\Psi = (Gr)^{\frac{1}{4}} Pr(4\xi)^{\frac{3}{4}} f(\xi, \eta),$$

and

$$\begin{aligned} &\eta = \left(\frac{Gr}{4\xi}\right)^{\frac{1}{4}} Y, \quad \theta(\xi, \eta) = \frac{T - T_\infty}{T_\mathrm{w} - T_\infty} \\ &\text{and} \quad T_\infty = T_\mathrm{w} - K, \end{aligned} \tag{10}$$

where $\xi = X$ and K is constant, the continuity equation (6) is automatically satisfied when a stream function Ψ is introduced, i.e.

$$U = \frac{\partial \Psi}{\partial Y} \quad \text{and} \quad V = -\frac{\partial \Psi}{\partial X}. \tag{11}$$

And the governing equations and the boundary conditions reduce to

$$f''' + 3ff'' - 2(f')^2 + \theta = 4\xi(f' f_{\xi\eta} - f_\xi f''), \tag{12}$$

$$\frac{1}{Pr}\theta'' + 3f\theta' = 4\,\xi(f'\theta_\xi - f_\xi\theta'), \tag{13}$$

subject to the boundary conditions

$$\begin{aligned} &\eta = 0: \quad f' = 0, \quad 3f + 4\xi f_\xi = \gamma\xi^{n+\frac{1}{4}}, \quad \theta = 1, \\ &\eta \to \infty: \ f' = \theta = 0, \end{aligned} \tag{14}$$

where $\gamma = \dfrac{-\sqrt{2}a}{(Gr)^{\frac{1}{4}}Pr}$ and the prime denotes the differentiation with respect to η.

2 HAM deformation equations

2.1 Zeroth-order deformation equation

According to the boundary condition (14), $f(\xi, \eta)$ and $\theta(\xi, \eta)$ can be expressed by the set of base function

$$\{\xi^n \eta^k \mathrm{e}^{-m\lambda\eta} |\ n \geqslant 0, \quad k \geqslant 0, \quad m \geqslant 0, \quad \lambda > 0\ \}$$

in the forms

$$f(\xi, \eta) = \sum_{m=0}^{\infty}\sum_{n=0}^{\infty}\sum_{k=0}^{\infty} a_{m,n}^k \xi^n \eta^k \mathrm{e}^{-m\lambda\eta}, \tag{15a}$$

$$\theta(\xi, \eta) = \sum_{m=0}^{\infty}\sum_{n=0}^{\infty}\sum_{k=0}^{\infty} b_{m,n}^k \xi^n \eta^k \mathrm{e}^{-m\lambda\eta}, \tag{15b}$$

where $a_{m,n}^k$, $b_{m,n}^k$ are the coefficients and $\lambda > 0$ is a scale parameter. These provide us the so-called solution expressions for $f(\xi, \eta)$ and $\theta(\xi, \eta)$. According to the solution expressions (15a) and (15b) and from the boundary conditions (14), it is convenient to choose

$$f_0(\xi, \eta) = \frac{2\mathrm{e}^{-\lambda\eta} - \mathrm{e}^{-2\lambda\eta} - 1}{\lambda} + \frac{\gamma\xi^{n+\frac{1}{4}}}{(4 + 4n)}, \tag{16a}$$

$$\theta_0(\xi, \eta) = \mathrm{e}^{-\lambda\eta}, \tag{16b}$$

as the initial approximations of $f(\xi, \eta)$ and $\theta(\xi, \eta)$, respectively. The original equations for $f(\xi, \eta)$ and $\theta(\xi, \eta)$ are third and second-order, respectively. So, we can choose the auxiliary linear operators

$$L_f = \frac{\partial^3}{\partial\eta^3} + a_2(\xi)\frac{\partial^2}{\partial\eta^2} + a_1(\xi)\frac{\partial}{\partial\eta} + a_0(\xi), \tag{17a}$$

$$L_\theta = \frac{\partial^2}{\partial\eta^2} + b_1(\xi)\frac{\partial}{\partial\eta} + b_0(\xi), \tag{17b}$$

where $a_0(\xi)$, $a_1(\xi)$, $a_2(\xi)$, $b_0(\xi)$ and $b_1(\xi)$ are real functions to be determined later. Let $w_1(\xi, \eta)$, $w_2(\xi, \eta)$ and $w_3(\xi, \eta)$ denote the three solutions of $L_f w = 0$, i.e.

$$\begin{aligned} &L_f[w_1(\xi, \eta)] = 0, \qquad L_f[w_2(\xi, \eta)] = 0, \\ &\text{and} \quad L_f[w_3(\xi, \eta)] = 0, \end{aligned} \tag{18}$$

according to the solution expression (15a) and the boundary condition (16b), we can choose

$$w_1 = 1, \quad w_2 = \exp(-\lambda\eta), \quad \text{and} \quad w_3 = \exp(\lambda\eta). \tag{19}$$

Substituting (19) into (18) with the definition (17a), we have the auxiliary linear operator

$$L_f = \frac{\partial^3 f}{\partial\eta^3} - \lambda^2\,\frac{\partial f}{\partial\eta}. \tag{20a}$$

In the similar way, we have

$$L_\theta = \frac{\partial^2\theta}{\partial\eta^2} - \lambda^2\theta. \tag{20b}$$

Note that

$$L_f[C_1 + C_2\mathrm{e}^{-\lambda\eta} + C_3\mathrm{e}^{\lambda\eta}] = 0, \tag{21a}$$

$$L_\theta[C_4 e^{-\lambda\eta} + C_5 e^{\lambda\eta}] = 0, \tag{21b}$$

where C_1, C_2, C_3, C_4 and C_5 are constants. Based on eqs. (12) and (13), we define the nonlinear operators

$$\begin{aligned} &N_f[\Phi(\xi,\eta;q)] \\ &= 4\xi\left[\frac{\partial\Phi(\xi,\eta;q)}{\partial\xi}\,\frac{\partial^2\Phi(\xi,\eta;q)}{\partial\eta^2} - \frac{\partial\Phi(\xi,\eta;q)}{\partial\eta}\,\frac{\partial^2\phi(\xi,\eta;q)}{\partial\xi\,\partial\eta}\right] \\ &\quad + \frac{\partial^3\Phi(\xi,\eta;q)}{\partial\eta^3} + 3\Phi\,\frac{\partial^2\Phi(\xi,\eta;q)}{\partial\eta^2} - 2\left(\frac{\partial\Phi(\xi,\eta;q)}{\partial\eta}\right)^2, \end{aligned} \tag{22}$$

$$\begin{aligned} &N_\theta[\Theta(\xi,\eta;q)] \\ &= 4\xi\Big[\frac{\partial\Phi(\xi,\eta;q)}{\partial\xi}\frac{\partial\Theta(\xi,\eta;q)}{\partial\eta} - \frac{\partial\Phi(\xi,\eta;q)}{\partial\eta}\frac{\partial\Theta(\xi,\eta;q)}{\partial\xi}\Big] \\ &\quad + \frac{1}{Pr}\frac{\partial^2\Theta(\xi,\eta;q)}{\partial\eta^2} + 3\Phi\frac{\partial\Theta(\xi,\eta;q)}{\partial\eta}. \end{aligned} \tag{23}$$

Let $\hbar_f$ and $\hbar_g$ denote the convergence-control parameters mentioned by Liao [34]. We construct the zeroth-order deformation equations

$$(1-q)L_f[\Phi(\xi,\eta;q) - f_0(\xi,\eta)] = q\hbar_f N_f[\Phi(\xi,\eta;q)], \tag{24a}$$

$$(1-q)L_\theta[\Theta(\xi,\eta;q) - \theta_0(\xi,\eta)] = q\hbar_g N_\theta[\Theta(\xi,\eta;q)], \tag{24b}$$

subject to the boundary conditions

$$\Phi_\eta(\xi,0;q) = 0, \qquad \Theta(\xi,0;q) = 1, \tag{25a}$$

$$\begin{aligned} &(1-q)\left[\Phi(\xi,0;q) - f_0(\xi,0)\right] \\ &\quad = q\hbar_b\left[3\Phi(\xi,0;q) + 4\xi\Phi_\xi - \gamma\xi^{n+\frac{1}{4}}\right], \end{aligned} \tag{25b}$$

$$\Phi_\eta(\xi,\infty;q) = 0, \qquad \Theta(\xi,\infty;q) = 0, \tag{25c}$$

where $q \in [0,1]$ is a homotopy-parameter. Obviously, when $q = 0$ and $q = 1$, the above zeroth-order deformation equations (24a) and (24b) have the solutions

$$\Phi(\xi,\eta;0) = f_0(\xi,\eta), \qquad \Theta(\xi,\eta;0) = \theta_0(\xi,\eta), \tag{26a}$$

and

$$\Phi(\xi,\eta;1) = f(\xi,\eta), \qquad \Theta(\xi,\eta;1) = \theta(\xi,\eta), \tag{26b}$$

respectively. Thus, as the homotopy-parameter q increases from 0 to 1, $\Phi(\xi,\eta)$ and $\Theta(\xi,\eta)$ vary from the initial guesses $f_0(\xi,\eta)$ and $\theta_0(\xi,\eta)$ to the solutions $f(\xi,\eta)$ and $\theta(\xi,\eta)$ of the considered problem, respectively. So, expanding $f(\xi,\eta)$ and $\theta(\xi,\eta)$ in Taylor's series with respect to q, we have

$$\Phi(\xi,\eta;q) = \Phi(\xi,\eta;0) + \sum_{m=1}^{+\infty} f_m(\xi,\eta)q^m, \tag{27a}$$

$$\Theta(\xi,\eta;q) = \Theta(\xi,\eta;0) + \sum_{m=1}^{+\infty} \theta_m(\xi,\eta)q^m, \tag{27b}$$

where

$$f_m(\xi,\eta) = \frac{1}{m!}\left.\frac{\partial^m\Phi(\xi,\eta;q)}{\partial q^m}\right|_{q=0},$$

$$\theta_m(\xi,\eta) = \frac{1}{m!}\left.\frac{\partial^m\Theta(\xi,\eta;q)}{\partial q^m}\right|_{q=0}.$$

Note that eqs. (24a) and (24b) contain the convergence-control parameters $\hbar_f$ and $\hbar_g$. Assuming that $\hbar_f$ and $\hbar_g$ are properly chosen so that the homotopy-series (27a) and (27b) are convergent at $q = 1$, we have, using eqs. (26a) and (26b), the homotopy-series solution

$$f(\xi,\eta) = f_0(\xi,\eta) + \sum_{m=1}^{+\infty} f_m(\xi,\eta), \tag{28a}$$

$$\theta(\xi,\eta) = \theta_0(\xi,\eta) + \sum_{m=1}^{+\infty} \theta_m(\xi,\eta). \tag{28b}$$

2.2 High-order deformation equation

For brevity, we define the vectors

$$\boldsymbol{f}_m = \{f_0(\xi,\eta), f_1(\xi,\eta), f_2(\xi,\eta), \cdots, f_m(\xi,\eta)\}, \tag{29a}$$

$$\boldsymbol{\theta}_m = \{\theta_0(\xi,\eta), \theta_1(\xi,\eta), \theta_2(\xi,\eta), \cdots, \theta_m(\xi,\eta)\}. \tag{29b}$$

Differentiating the zeroth-order deformation equations (24a) and (24b) m-times with respect to the homotopy-parameter q and dividing the resulting expression by $m!$ and then setting $q = 0$, we have the mth-order deformation equations

$$L_f[f_m(\xi,\eta) - \chi_m f_{m-1}(\xi,\eta)] = \hbar_f R_m(\boldsymbol{f}_{m-1}), \tag{30a}$$

$$L_\theta[\theta_m(\xi,\eta) - \chi_m\theta_{m-1}(\xi,\eta)] = \hbar_g S_m(\boldsymbol{\theta}_{m-1}), \tag{30b}$$

subject to the boundary conditions

$$\theta_m(0,\xi) = \left.\frac{\partial f_m}{\partial\eta}\right|_{\eta=0} = 0, \tag{31a}$$

$$\begin{aligned} f_m - \chi_m\, f_{m-1} =& \hbar_b\Big[3f_{m-1} + 4\xi\,\frac{\partial f_{m-1}}{\partial\xi} \\ &- \gamma\xi^{n+\frac{1}{4}}(1-\chi_m)\Big], \end{aligned} \tag{31b}$$

$$\theta_m(\infty,\xi) = \left.\frac{\partial f_m}{\partial\eta}\right|_{\eta\to+\infty} = 0, \tag{31c}$$

where

$$R_m(\boldsymbol{f}_{m-1}) = \frac{1}{(m-1)!}\left.\frac{\partial^{m-1}N_f[\Phi(\xi,\eta;q)]}{\partial q^{m-1}}\right|_{q=0}, \tag{32a}$$

$$S_m(\boldsymbol{\theta}_{m-1}) = \frac{1}{(m-1)!}\left.\frac{\partial^{m-1}N_\theta[\Theta(\xi,\eta;q)]}{\partial q^{m-1}}\right|_{q=0}, \tag{32b}$$

and

$$\chi_m = \begin{cases} 0, & m \leqslant 1, \\ 1, & m > 1. \end{cases} \tag{33}$$

Let $f^*(\xi,\eta)$ and $\theta^*(\xi,\eta)$ denote the particular solutions of (30a) and (30b). Using eqs. (21a) and (21b), we have the general solutions

$$f_m(\xi,\eta) = f_m^*(\xi,\eta) + C_1 + C_2 e^{-\lambda\eta}, \tag{34a}$$

$$\theta_m(\xi,\eta) = \theta_m^*(\xi,\eta) + C_4 \mathrm{e}^{-\lambda\eta}, \tag{34b}$$

where

$$f_m^*(\xi,\eta) = \chi_m\, f_{m-1}(\xi,\eta) + \hbar_f\, L_f^{-1}\,[R_m(\boldsymbol{f}_{m-1})],$$

$$\theta_m^*(\xi,\eta) = \chi_m\, \theta_{m-1}(\xi,\eta) + \hbar_g\, L_\theta^{-1}\,[S_m(\boldsymbol{\theta}_{m-1})],$$

and

$$C_1 = -C_2 - f_m^*(\xi,0) + \chi_m f_{m-1}(\xi,0) + \hbar_b\left[3f_{m-1}(\xi,0) + 4\xi\frac{\partial f_{m-1}(\xi,0)}{\partial\xi} - \gamma\xi^{n+\frac{1}{4}}(1-\chi_m)\right],$$

$$C_2 = \frac{1}{\lambda}\left.\frac{\partial f_m^*}{\partial\eta}\right|_{\eta=0}, \qquad C_4 = -\theta_m^*(\xi,0),$$

where L_f^{-1} and L_θ^{-1} are inverse operators of L_f and L_θ, respectively. In this way, it is easy to solve the systems of linear PDEs (30a) and (30b) by means of the symbolic computation software such as Mathematica, Matlab and Maple.

The quantities of physical interest are the skin friction coefficient C_f and the local Nusselt number Nu_x, defined respectively by

$$C_\mathrm{f} = \frac{2\tau_w}{\rho u_c^2}, \quad Nu_x = \frac{L\dot{q}_w}{k(T_w - T_\infty)}, \tag{35}$$

where ρ is the fluid density. The wall shear stress τ_w and the surface heat flux $\dot{q}_\mathrm{w}$ are given by

$$\tau_\mathrm{w} = \mu\left.\frac{\partial u}{\partial y}\right|_{y=0}, \quad \dot{q}_\mathrm{w} = -k\left.\frac{\partial T}{\partial y}\right|_{y=0}, \tag{36}$$

where μ and k are the dynamic viscosity and thermal conductivity, respectively. Using the dimensionless quantities (10), we obtain

$$C_\mathrm{f} = \frac{2\,Gr^{\frac{3}{4}}\,(4\xi)^{\frac{1}{4}}}{\sqrt{Re_x}}\left.\frac{\partial^2 f}{\partial\,\eta^2}\right|_{\eta=0}, \quad Nu_x = \frac{-Gr^{\frac{1}{4}}}{(4\xi)^{\frac{1}{4}}}\left.\frac{\partial\,\theta}{\partial\,\eta}\right|_{\eta=0}. \tag{37}$$

3 Results and analysis

The nonlinear coupled PDEs (12) and (13) with the boundary condition (14) have been solved analytically by using the homotopy analysis method. Note that the homotopy-series solution (28a) and (28b) contain three convergence-control parameters $\hbar_f$, $\hbar_g$ and $\hbar_b$. For simplicity, we take here $\hbar_b = \hbar_f$. Note that n is the injection index and γ is related to the injection velocity $V_w(x)$ through the constant a. Note that $\gamma > 0$ when a is negative (suction), and $\gamma < 0$ when a is positive (injection).

Without loss of generality, let us consider the case of $\gamma > 0$, and check the influence of λ, $\hbar_g$ and $\hbar_f$ on the homotopy-series solution of $f''(\xi,0)$ and $\theta'(\xi,0)$. First, we set $\hbar_f = \hbar_g = -1$ so that the homotopy-series solution only depends on λ, and then we investigate the influence of λ on $f''(\xi,0)$ by plotting the curves of $f''(\xi,0) \sim \lambda$. It is found that, when $\lambda \geqslant 5$, the series $f''(\xi,0)$ converges to the same value as shown in Figure 1. Secondly, we set $\lambda = 5$ and regard $\hbar_f = \hbar_g = \hbar$ as a unknown variable. As Liao [23,35] proved in general that, as long as a homotopy-series solution given by the homotopy analysis method is not divergent, it must converge to the exact solution of original nonlinear problems under investigation. Note that now the homotopy-series solutions (28a) and (28b) contain the convergence-control parameters $\hbar$, which influences the convergence of the homotopy-series (28a) and (28b). Thus, mathematically, the series solutions are dependent upon $\hbar$. But, physically, the solution is independent of the convergence-control parameters $\hbar$. As a result, the homotopy-series must converge to the same result for all corresponding values of $\hbar$ which ensures the convergence. As mentioned by Liao [23], the admissible values of $\hbar$ for which the homotopy-series converges can be determined by plotting the so-called $\hbar$-curves or by plotting the residual error verses $\hbar$. Let $\delta_m(\xi,\eta)$ denotes the residual error of the mth-order homotopy-series approximation, and $\Delta = \int\int \delta_m^2(\xi,\eta)\mathrm{d}\xi\mathrm{d}\eta$ denote the integral of the residual error. Plotting the curves of $\Delta \sim \hbar$, it is straight forward to find a region of $\hbar$ in which Δ decreases to zero as the order of approximation increases. In this way, we can get the best value of $\hbar$ corresponding to the minimum of the residual error of the original governing equation. For example, when given λ, n, and Pr, the approximate region for the convergence of the homotopy-series is about $-8/5 \leqslant \hbar \leqslant -1/2$ as shown in Figure 2. In a similar way, we can investigate the so-called $\hbar$-curves for $\theta'(\xi,0)$ which has important physical meanings.

In general, we can substitute the series solutions for the governing equations and evaluate the square residual error so as to check the convergence of the solutions. Table 1 shows the square residual error of eqs. (12) and (13). It is seen that

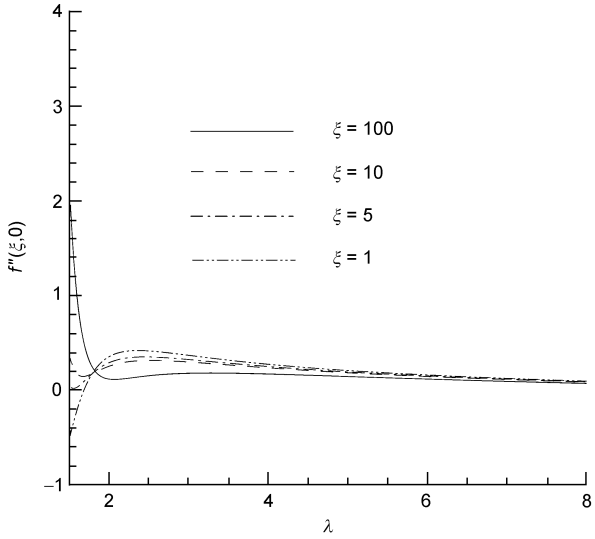

Figure 1 The 15th-order approximation of $f''(\xi,0)$ when $n = 0$, $Pr = 7$, $\gamma = 1/4$ by means of $\hbar_f = -1$ and $\hbar_g = -1$.

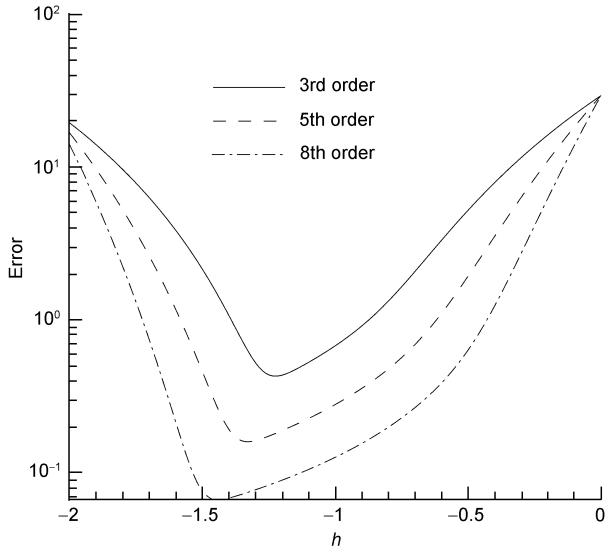

Figure 2 Square residual error of $f(\xi,\eta)$ verses convergence-control parameter $\hbar$ when $n = 0$, $Pr = 7$, and $\gamma = 1/4$ by means of $\lambda = 5$.

Table 1 Square residual error of $f(\xi,\eta)$ eq. (12) and $\theta(\xi,\eta)$ eq. (13) when $Pr = 7$, $n = 0$, and $\gamma = 1/4$ by means of $\hbar_f = -1$, $\hbar_g = -4/5$, and $\lambda = 5$

Order of approximation	Residual error of $f(\xi,\eta)$	Residual error of $\theta(\xi,\eta)$
1st	3.89014	0.26386
5th	0.27906	0.17008
10th	0.08693	0.11951
15th	0.04585	0.08624

by increasing the order of approximation the square residual error decreases. This indicates that our HAM series solution is convergent. Besides, the so-called homotopy-Padé technique [23] is used to accelerate the convergence of the homotopy-series solution. In the current study, we compared [14,14] homotopy-Padé approximations with [18,18] homotopy-Padé approximations and found very good agreement.

In many practical applications, the heat transfer rate at the surface, are vital since they influence the quality of the final products. Figure 3 shows the heat transfer parameter for various values of Prandtl number (Pr) when the other physical parameters are fixed. It is evident from Figure 3 that the heat transfer parameter at the surface increases as Pr increases. This is because the fluid with higher Prandtl number has a relatively low thermal conductivity, which reduces conduction, and thereby reduces the thermal boundary-layer thickness, and as a consequence, increases the heat transfer rate at the surface. On the other hand as shown in Figure 3 the local skin friction coefficient decreases with the increase of Pr. The reason is that fluid of the higher Prandtl number means more viscous fluid, which increases the boundary-layer thickness and thus, reduces the shear stress. As a whole, it may be pointed out that the effect of Pr is more pronounced on the Nusselt number $(Nu_x/(Gr)^{1/4})$ as compared to the skin friction coefficient $(C_f\sqrt{Re_x}/(Gr)^{3/4})$. It is also observed from Figures 3 and 4 that the similarity solution exists as $\xi \to 0$ and $\xi \to \infty$. However, the flows in the region $0.5 \leqslant \xi \leqslant 10$ are non-similar. Thus, the non-similarity flows in the region $\xi \to 0$ and $\xi \to \infty$ are very close to the similarity ones for all Prandtl numbers Pr.

Figures 5 and 6 represent the effect of the parameter γ on the local Nusselt number for $n = 0$, and $\lambda = 5$ for $Pr = 0.72$

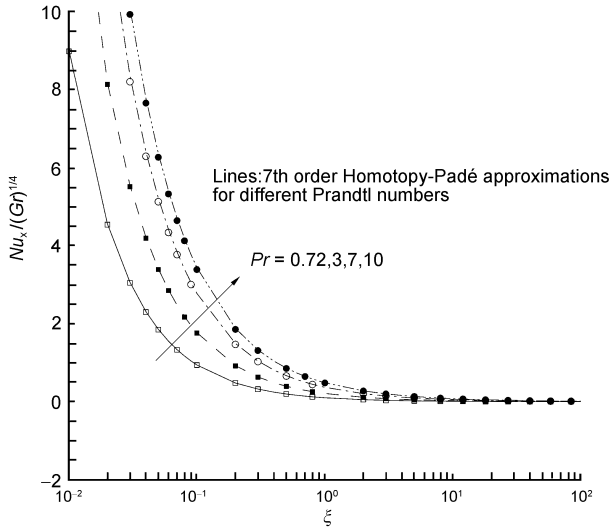

Figure 3 The 9th-order homotopy-Padé approximation of Local Nusselt number $Nu_x/(Gr)^{1/4}$ for different Prandtl numbers when $n = 0$, $\gamma = 1/4$ by means of $\hbar_f = -1$, $\hbar_g = -4/5$ and $\lambda = 5$. Squares: $Pr = 0.72$; filled squares: $Pr = 3$; circles: $Pr = 7$; filled circles: $Pr = 10$.

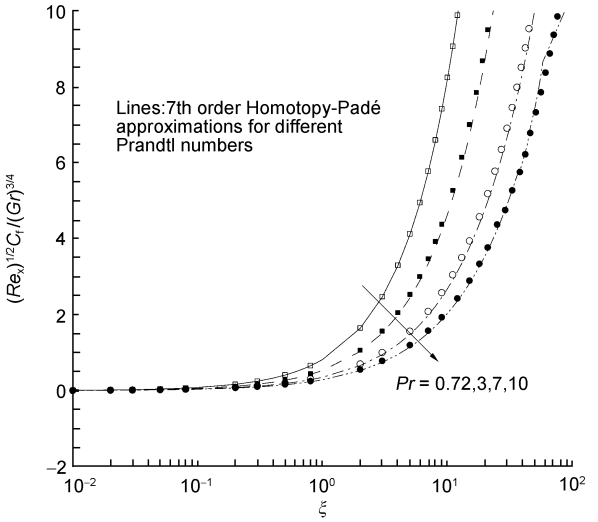

Figure 4 The 9th-order homotopy-Padé approximation of skin friction coefficient $C_f\sqrt{Re_x}/(Gr)^{3/4}$ for different Prandtl numbers when $n = 0$, $\gamma = 1/4$ by means of $\hbar_f = -1$, $\hbar_g = -4/5$ and $\lambda = 5$. Squares: $Pr = 0.72$; filled squares: $Pr = 3$; circles: $Pr = 7$; filled circles: $Pr = 10$.

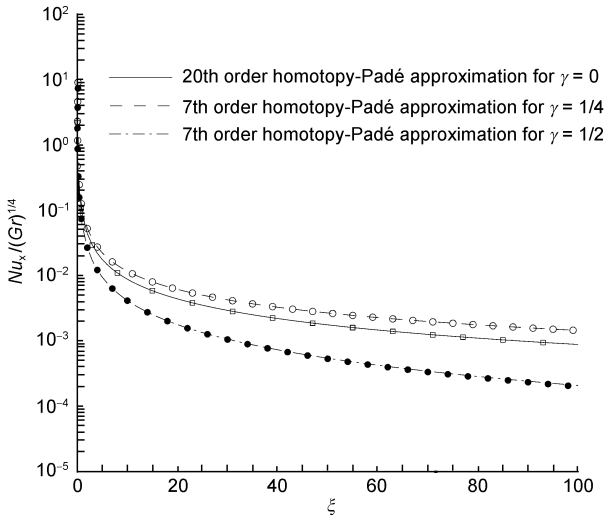

Figure 5 The influence of γ on the Local Nusselt number $Nu_x/(Gr)^{1/4}$ when $n = 0$, $Pr = 0.72$ by means of $\lambda = 5$. Squares: [22,22] homotopy-Padé approximation for $\gamma = 0$ by means of $\hbar_f = \hbar_g = -1$; circles: [9,9] homotopy-Padé approximation for $\gamma = 1/4$ by means of $\hbar_f = -1$ and $\hbar_g = -4/5$; filled circles: [9,9] homotopy-Padé approximation for $\gamma = -1/2$ by means of $\hbar_f = -1$ and $\hbar_g = -4/5$.

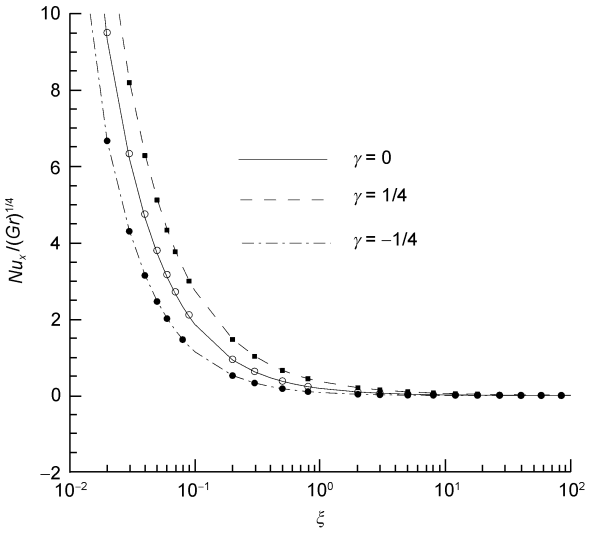

Figure 6 The influence of γ on the Local Nusselt number $Nu_x/(Gr)^{1/4}$ when $n = 0$, $Pr = 7$ by means of $\lambda = 5$. Solid line: [22,22] homotopy-Padé approximation for $\gamma = 0$ by means of $\hbar_f = \hbar_g = -1$; dashed line: [10,10] homotopy-Padé approximation for $\gamma = 1/4$ by means of $\hbar_f = -1$ and $\hbar_g = -4/5$; dash-dotted line: [8,8] homotopy-Padé approximation for $\gamma = -1/4$ by means of $\hbar_f = -1$ and $\hbar_g = -4/5$; squares: [20,20] homotopy-Padé approximation for $\gamma = 0$; open circles: [8,8] homotopy-Padé approximation for $\gamma = 1/4$; filled circles: [6,6] homotopy-Padé approximation for $\gamma = -1/4$.

and $Pr = 7$ for air and water, respectively. It is clear from the figures that the heat transfer rate at the surface is higher for suction ($\gamma > 0$), as compared to the injection ($\gamma < 0$). This is due to the fact that the surface shear stress increases when introducing suction, which in turn increases the local Nusselt number. The heat transfer parameter increase significantly with the Prandtl number, as higher Prandtl number has lower thermal conductivity, which results in thinner thermal boundary-layer and, hence, a higher heat transfer rate at the wall.

The influence of the suction/injection parameter on the skin friction coefficient can be seen from Figures 7 and 8 for water and air, respectively. It is observed that at the low Prandtl number the suction increases the skin friction while at the high Prandtl number it decreases. On the other hand, the effect of injection is just the opposite. This is due to the fact that the higher Prandtl number implies more viscous fluid which increases the boundary-layer thickness and consequently, reduces the skin friction coefficient. It is also clear from Figures 6 and 7, that the non-similarity flows in the region $\xi \to 0$ and $\xi \to \infty$ are very close to the similarity ones for the suction/injection parameter γ. However, the flows in the region $0.5 \leqslant \xi \leqslant 10$ are non-similar. The same phenomenon is observed for negative values of the n.

4 Conclusion

The present paper deals with the effect of the suction/injection parameter γ, and the Prandtl number Pr, on the laminar free convection boundary-layer flow from a permeable verti-

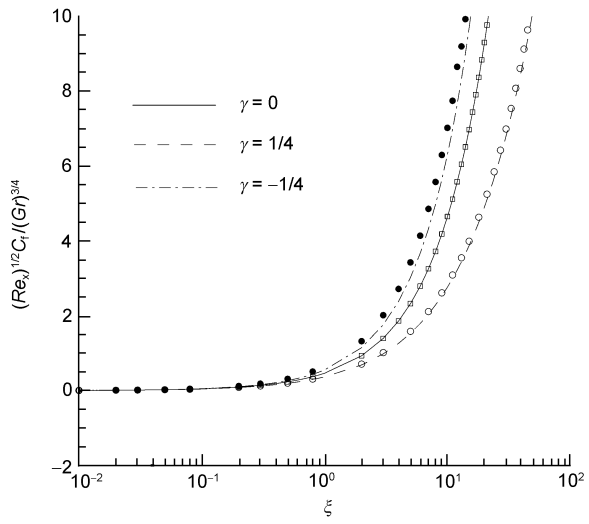

Figure 7 The influence of γ on the skin friction coefficient $C_f\sqrt{Re_x}/(Gr)^{3/4}$ when $n = 0$, $Pr = 7$ by means of $\lambda = 5$. Solid line: [22,22] homotopy-Padé approximation for $\gamma = 0$ by means of $\hbar_f = \hbar_g = -1$; dashed line: [10,10] homotopy-Padé approximation for $\gamma = 1/4$ by means of $\hbar_f = -1$ and $\hbar_g = -4/5$; dash-dotted line: [8,8] homotopy-Padé approximation for $\gamma = -1/4$ by means of $\hbar_f = -1$ and $\hbar_g = -4/5$; squares: [20,20] homotopy-Padé approximation for $\gamma = 0$; open circles: [8,8] homotopy-Padé approximation for $\gamma = 1/4$; filled circles: [6,6] homotopy-Padé approximation for $\gamma = -1/4$.

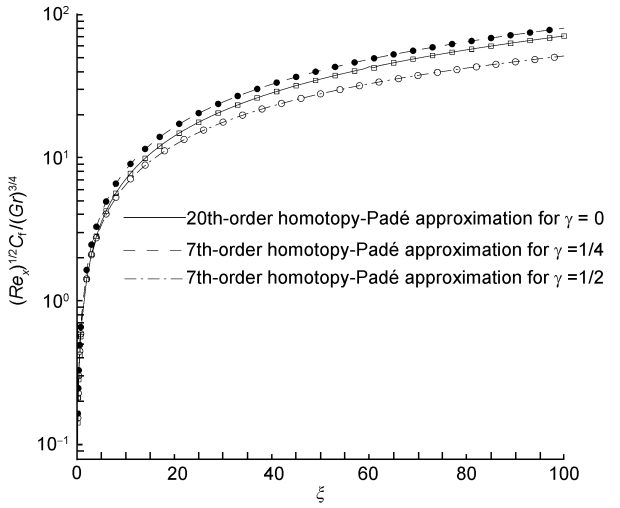

Figure 8 The influence of γ on the skin friction coefficient $C_{\rm f}\sqrt{Re_x}/(Gr)^{3/4}$ when $n = 0$, $Pr = 0.72$ by means of $\lambda = 5$. Squares: [22,22] homotopy-Padé approximation for $\gamma = 0$ by means of $\hbar_f = \hbar_g = -1$; filled circles: [9,9] homotopy-Padé approximation for $\gamma = 1/4$ by means of $\hbar_f = -1$ and $\hbar_g = -4/5$; circles: [9,9] homotopy-Padé approximation for $\gamma = -1/2$ by means of $\hbar_f = -1$ and $\hbar_g = -4/5$.

cal surface in isothermal surroundings. The governing non-similarity boundary-layer equations for flow and temperature fields are solved using the homotopy analysis method. And the so-called homotopy-Padé technique is applied to accelerate the convergence. The results are expressed in terms of the local skin friction and the local Nusselt number. Different from the previous analytic results, our homotopy-series solutions are convergent and valid for all physical parameters in the whole domain $0 \leqslant x < \infty$ and $0 \leqslant y < \infty$. To the best of our knowledge, such kind of convergent series solution has never been reported. Mathematically, this analytic approach has general meanings and can be applied to solve many other non-similarity boundary-layer flows in fluid mechanics.

Physically, from the present investigations, it may be concluded:

(1) An increase in the value of Prandtl number Pr, leads to the decrease in the value of the skin friction coefficient. However, the local Nusselt number increases with the increasing of Prandtl number Pr.

(2) Suction parameter increases the local Nusselt number for both $Pr = 0.72$ and $Pr = 7$, corresponding to air and water, respectively. On the other hand, the injection has just the opposite effect.

(3) Suction increases the local skin friction for lower Prandtl number 0.72 while decreases the value of local skin friction for higher Prandtl number 7. But in the case of injection, the effect of Prandtl number is opposite on the value of the local skin friction.

(4) The similarity solution exist for $\xi \leqslant 0.5$ and $\xi \geqslant 10$. On the other hand, the solution is non-similar in the region $0.5 \leqslant \xi \leqslant 10$ for all the values of Prandtl numbers Pr and the suction/injection parameter γ.

This work is partly supported by National Natural Science Foundation of China (Grant No. 10872129) and State Key Lab of Ocean Engineering (Grant No. GKZD010002).

1 Cheesewright R. Natural convection from a plane vertical surface in non-isothermal surroundings. Int J Heat Mass Transfer, 1967, 10: 1847–1859
2 Eichhorn R. Natural convection in a thermally stratified fluid. Prog Heat Mass Transfer, 1969, 2: 41–53
3 Fujii T, Takeuchi M, Morioka I. Laminar boundary-layer of free convection in a temperature stratified environment. In: Proceedings of the Fifth International heat transfer Conference, Tokyo, NC2., 1974, 2: 44–48
4 Chen C C, Eichhorn. Natural convection from a vertical surface to a thermally stratified fluid. ASME J heat transfer, 1976, 98: 446–451
5 Yang K T, Novotny J L, Chang Y S. Laminar free convection from a non-isothermal plate immersed in a temperature stratified medium. Int J Heat Mass Transfer, 1972, 15: 1097–1109
6 Venkatachala B J, Nath G. Non-similar laminar natural convection in a thermal stratified fluid. Int J Heat Mass Transfer, 1981, 11: 1848–1850
7 Jaluria Y, Himasekhar K. Buoyancy-induced two-dimensional vertical flows in a thermally stratified fluid. J Comput Fluids, 1983, 11: 39–49
8 Kulkarni A K, Jacobs H R, Hwang J J. Similarity solutions for natural convection flow over an isothermal wall immersed in thermally stratified medium. Int J Heat Mass Transfer, 1986, 4: 691–698
9 Tanny J, Cohen J. The mean temperature field of a buoyancy-induced boundary layer adjacent to a vertical plate immersed in a stratified medium. Int J Heat Mass Transfer, 1998, 41: 2125–2130
10 Kao T T. Laminar incompressible forced convection along a flat plate with arbitrary suction or injection at the wall. Trans ASME, 1975, 484–486
11 Emmons H W, Leigh D C. Tabulation Blasius function with blowing and suction. Aero Nautical Research Council Current Papers, 1954. C.P.N 157
12 Schlichting H, Bussemann K. Exakte losengen fur die laminar grenzschieht mit absaugu der absblasen. Sorgruften der deutschen akert der luftfahrt-forschung B, 1943, 2: 1
13 Wanous K J, Sparrow E M. Heat transfer for flow longitudinal to a cylinder with surface mass transfer. Heat Transfer Trans Ser C, 1965, 87: 317–319
14 Catherall D, Stewartson W. Viscous flow past a flat plate with uniform injection. Proc R Soc A, 1965, 284: 370–396
15 Cimpean D, Merkin J H, Ingham D B. On a free convection problem over a vertical flat surface in a porous medium. Transport Porous, 2006, 64: 393–411
16 Sparrow E M, Quack H, Boerner C J. Local non-similarity boundary layer solutions. J AIAA, 1970, 8: 1936–1942
17 Sparrow E M, Yu H S. Local non-similarity thermal boundary-layer solutions. J Heat Transfer Trans ASME, 1971, 328–334
18 Massoudi M. Local non-similarity solutions for the flow of a non-Newtonian fluid over a wedge. Int J Non-Linear Mech, 2001, 36: 961–976
19 Nayfeh A H. Perturbation Methods. New York: John Wiley and Sons, 2000
20 Lyapunov A M. General Problem on Stability of Motion. (English translation), London: Taylor and Francis, 1992 (Original work published 1892)

21 Karmishin A V, Zhukov A I, Kolosov V G. Methods of Dynamics Calculation and Testing for Thin-Walled Structures. Moscow: Mashinostroyenie, 1990 (in Russian)
22 Adomian G. Solving Frontier Problems of Physics: The Decomposition Method. Boston and London: Kluwer Academic Publishers, 1994
23 Liao S J. Beyond perturbation: Introduction to the homotopy analysis method. Boca Raton: Chapman and Hall/CRC Press, 2003
24 Abbasbandy S. Homotopy analysis method for heat radiation equations. Int Commun Heat Mass Transfer, 2007, 34: 380–387
25 Abbasbandy S. The application of homotopy analysis method to nonlinear equations arising in heat transfer. Phys Lett A, 2006, 360: 109–113
26 Sajid M, Hayat T. Comparison of HAM and HPM methods for nonlinear heat conduction convection equations. Nonlinear Anal, 2008, 9: 2296–2301
27 Zhu S P. A closed-form analytical solution for the valuation of convertible bonds with constant dividend yield. ANZIAM J, 2006, 47: 477–494
28 Zhu S P. An exact and explicit solution for the valuation of American put options. Quant Finan, 2006, 6: 229–242
29 Yamashita M, Yabushita K, Tsuboi K. An analytic solution of projectile motion with the quadratic resistance law using the homotopy analysis method. J Phys A, 2007, 40: 8403–8416
30 Song H, Tao L. Homotopy analysis of 1D unsteady, nonlinear groundwater flow through porous media. J Coastal Res, 2007, 50: 292–295
31 Cai W H. Nonlinear Dynamics of thermal-hydraulic networks. Dissertation for the Doctoral Degree. Indiana: University of Notre Dame, 2006
32 Liao S J. A new branch of solutions of boundary-layer flows over an impermeable stretched plate. Int J Heat Mass Transfer, 2005, 48: 2529–2539
33 Liao S J, Magyari E. Exponentially decaying boundary layers as limiting cases of families of algebraically decaying ones. ZAMP, 2006, 57: 777–792
34 Liao S J. Notes on the homotopy analysis method: Some definitions and theorems. Commun Nonlinear Sci Numer Simulat, 2009, 14: 983–997
35 Liao S J. The proposed homotopy analysis technique for the solution of nonlinear problems. Dissertation for the Doctoral Degree. Shanghai: Shanghai Jiao Tong University, 1992